doi:10.1017/S1431927615010983 Paper No. 1019 Microsc. Microanal. 21 (Suppl 3), 2015

Automated Dictionary-based Indexing of Electron Channeling Patterns

Saransh Singh[1], Marc De Graef[1]

[1] Dept. of Materials Science and Engineering, Carnegie Mellon Univ., Pittsburgh PA 15213, USA

Traditionally, crystal defects (dislocations, stacking faults etc.) have been studied using TEM image modalities, such as bright field-dark field, weak beam, and STEM diffraction contrast imaging. Although these techniques offer high spatial resolution, they suffer from a number of drawbacks: tedious sample preparation; limited available thin area; and lack of a guarantee that the defect remains identical to that found in bulk crystals. Electron Channeling Contrast Imaging (ECCI) has recently gained visibility as a technique for the study of near surface defects in crystals [1]. ECCI is an SEM image modality (which hence enjoys less demanding sample preparation requirements) and relies on the variation of the backscattered electron yield near crystal defects. It has been shown that the burgers vector of a surface penetrating dislocation can be identified using the same visibility criteria as used in the TEM. The ECCI technique, however, requires accurate knowledge of the diffraction conditions, which, in turn, requires determination of the crystal orientation. While Electron Back Scatter Diffraction (EBSD) can be used to determine the sample/grain orientation, it would be more convenient to have the ability to determine the orientation from an Electron Channeling Patterns (ECPs), since such patterns are acquired already as part of an ECCI observation. While there are several commercial packages available for the indexing of EBSD patterns, no such counterpart exists for ECPs.

In this contribution, we introduce a dictionary based approach to index ECPs, based on previous work with EBSD pattern indexing [2]. The dictionary approach uses a physics-based forward model, described in detail in [3], to generate a set of simulated ECPs, utilizing the microscope geometrical parameters and symmetry information of the crystal being studied. The forward model estimates the depth distribution of the BSE1-type electrons using a Monte Carlo approach, and then integrates the backscatter probability over the corresponding depth range for electron exit directions sampled on a sphere. Details of the simulations, which can be performed using either Bloch waves or the scattering matrix formalism, can be found in [3]. This forward model is used to compute a so-called "master" channeling pattern, from which any ECP can be interpolated using bi-linear interpolation. The simulated master pattern for Nickel for a 30 kV acceleration voltage is shown in Fig. 1(a) using a modified equal-area Lambert projection from the hemisphere to a square. Fig. 1(b) shows the $[001]$ zone axis pattern interpolated from the master pattern. Several representative dictionary patterns interpolated from the master pattern, along with the corresponding Euler angles, are shown in Fig. 2(a)-(e).

In the dictionary approach, each ECP is reformatted as a normalized column vector (with or without average background subtracted), and the dot products between each experimental ECP and all dictionary pattern vectors are computed and ranked in decreasing order. The top k dot products (typically, $k = 40$ or so) and their associated Euler angles are kept for further analysis; this set of k patterns represents the k-nearest-neighbor (kNN) neighborhood of the experimental pattern in the dictionary. Cluster analysis of this neighborhood and the kNN neighborhoods of neighboring pixels provides information on whether the experimental pattern likely stems from a grain interior region or from a region close to a grain boundary. The Euler angle estimation of the lattice orientation at a particular pixel is performed using a directional statistics analysis [4] of the top k inner product matches. Since orientations can be mapped onto unit quaternions on the unit sphere S^3 in $\mathbb{R}^4$, one must use 4D directional distribution functions; both the von Mises-Fisher (vMF) distribution and the axial Watson distribution have been

found to be useful in this respect; they are defined by

$$f_{\text{vMF}}(\mathbf{x};\boldsymbol{\mu},\kappa) = c_{\text{vMF}}(\kappa)\mathrm{e}^{\kappa\boldsymbol{\mu}\cdot\mathbf{x}}, \quad f_{\text{Watson}}(\mathbf{x};\boldsymbol{\mu},\kappa) = c_{\text{Watson}}(\kappa)\mathrm{e}^{\kappa(\boldsymbol{\mu}\cdot\mathbf{x})^2};$$

$\boldsymbol{\mu}$ is the quaternion representing the mean direction, $\mathbf{x}$ is a unit quaternion, and κ is the concentration parameter (a measure for the spread of the distribution); the normalization factors are given by $c_{\text{vMF}}(\kappa) = \kappa/(4\pi^2 I_1(\kappa))$ and $c_{\text{Watson}}(\kappa) = \exp(-\kappa/2)/(I_0(\kappa/2) - I_1(\kappa/2))$, with $I_i(x)$ a modified Bessel function of order i. For a given kNN, the corresponding unit quaternions are used in a Maximum Likelihood (ML) estimation framework to determine the most likely mean direction $\boldsymbol{\mu}$ and concentration parameter κ for each experimental ECP. The ML approach uses mixtures of vMF or Watson distributions, and explicitly takes crystallographic symmetry into account. The approach has been implemented on a combination of multi-core CPUs and a GPU to maximize performance. We will present ECP indexing results as well as an analysis of the robustness of the dictionary approach.

References

[1] D.R. Clarke, Philosophical Magazine **24** (1971) p. 973.
[2] Y.H. Chen *et al*, Microscopy and Microanalysis, under review.
[3] P.G. Callahan and M. De Graef, Microscopy and Microanalysis **19** (2013) p. 1255.
[4] K.V. Marida and P.E. Jupp, "Directional Statistics," Wiley & Sons (1999).
[5] Research supported by the Air Force Office of Scientific Research, MURI contract # FA9550-12-1-0458.

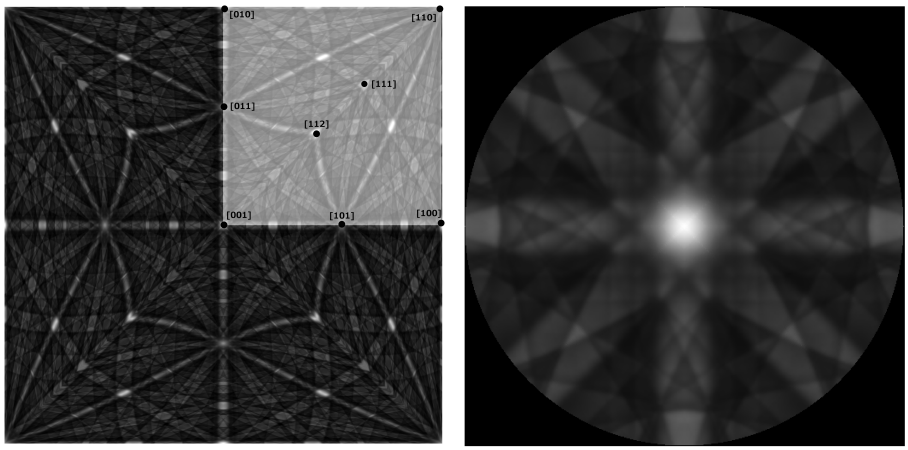

(a) (b)

Figure 1: (a) Modified equal-area Lambert projection of the ECP master pattern for Ni at 30 kV. The top right quadrant is deliberately made lighter to show some prominent zone axis. (b) shows the $[001]$ zone axis pattern for an angular range of 8^{o} interpolated from the master pattern.

(a) (63.08,47.39, 333.08) (b) (62.33,48.47,332.33) (c) (61.56,49.51,331.56) (d) (60.75,50.51,330.75) (e) (59.92,51.46,329.92)

Figure 2: (a)-(e) Simulated ECPs for different Bunge Euler angles; Nickel, 30 keV.